Bandstop Filter Design Using a Dielectric Waveguide Grating

DONG CHUL PARK, MEMBER, IEEE, GEORGE L. MATTHAEI, FELLOW, IEEE, AND MU SHENG WEI

Abstract — **Precision design techniques are obtained for dieletric waveguide (DW) bandstop filters with bandwidths up into the 5–10-percent range. Dielectric waveguide bandstop filters are realized in the form of a grating in the DW image guide which utilizes notches of varying depth and length. The grating is designed from a transmission-line prototype which has a prescribed stopband and also prescribed Chebyshev passbands. An approximate synthesis procedure for such prototypes is presented. Design data for grating notches were obtained from tests on uniform gratings, while DW dispersion is compensated for by calculations based on the "effective dielectric constant" method. Excellent agreement between computed and measured attenuation response is obtained. Two such grating structures used with loads on one end and a 3-dB coupler can be used to form a bandpass filter.**

I. Introduction

DIELETRIC WAVEGUIDE (DW) gratings with uniformly periodic notches can be used as millimeter-wave or optical-frequency bandstop filters [1],[2]. Though such uniform gratings can give a strong stopband, their passbands may have ripples of the order of two decibels or so, which is excessive for many applications. In order to obtain Chebyshev passbands with a prescribed low level of ripple, we require gratings with notches of varying depth and length. In Fig. 2, a typical attenuation characteristic is shown for a bandstop filter of this type. This kind of DW bandstop filter can give stopband widths to the equal-ripple points up into the 10-percent range.

Some part of this work has been described in [3]. Herein, we will discuss in more depth a systematic design procedure for the above-mentioned type of bandstop filter, and a simple procedure for approximate correction of the effects of DW dispersion. Illustrative theoretical and experimental results will also be presented.

II. Characterization of the Gratings

The DW gratings we have used in our experimental work are of the image-guide type with grating notches on the sides of the guide as shown in Fig. 1. The length of each notched and unnotched region of the grating in Fig. 1 is approximately a quarter guide wavelength at the center of the grating stopband. We have found gratings of this type to be advantageous when using the lowest order mode which has its E-field predominantly vertically polarized. For that mode, notches on the sides give stronger stopband attenuation with no nearby spurious responses. However, if the lowest order horizontally polarized mode is used, notches on the top of the guide are most effective, and for some applications that arrangement may be desirable.

We have found that we can model gratings with good accuracy by use of an equal-line-length transmission-line equivalent circuit as is shown in Fig. 3(a) with a frequency-dependent velocity introduced to account for dispersion [2]. The equal-line-length transmission-line model with appropriate parameters can also be applied to represent a grating accurately over a wide band of frequencies even if the electrical lengths of the grating notched and unnotched sections are fairly unequal [2]. This works provided appropriate *effective* values of wave velocity and impedance ratio r are used in the equal-line-length model.

In order to carry out trial designs such as are described later in this paper, it is useful to have accurate data for the effective ratios of the impedances of the notched regions to those of the unnotched region of *uniformly* periodic gratings so that in Fig. 1 all notched section widths equal w_1 and all lengths of notched and unnotched sections are $l_0 = l_1 = l_i = l$. Also, data is desired for the effective average wave velocity, which is ascertained from the frequency f_0' at which the mid-stopband attenuation A_{max} occurs in the grating. (For a uniform grating, a response similar to that in Fig. 2 is obtained but with unequal ripples. The largest ripples are adjacent to the stopband. Here, f_0' is used for the stopband center frequency for a uniform grating, while f_0 is used for the stopband center of the desired Chebyshev designs.) A uniform grating can be modeled by an equal-line-length transmission-line circuit as in Fig. 3(b) with all primed impedances equal to Z_1 (the impedance for the notched regions). As presented in our previous paper [2], we can compute the impedance ratio $r = Z_1/Z_0$ for use in the equal-line-length model from a measured value of A_{max} (in decibels) for a test grating using the equation

$$r = \sqrt[2n']{\frac{1+\sqrt{(1-T)}}{1-\sqrt{(1-T)}}} = \frac{Z_1}{Z_0} > 1 \qquad (1a)$$

Manuscript received October 17, 1984; revised March 29, 1985. This work was supported in part by the National Science Foundation under Grants ECS80-16720 and ECS83-11987.

D. C. Park was with the Department of Electrical and Computer Engineering, University of California, Santa Barbara, CA. He is now with the Department of Electronics Engineering, Chungnam National University, Daejon, South Korea.

G. L. Matthaei and M. S. Wei are with the Department of Electrical and Computer Engineering, University of California, Santa Barbara, CA 93106.

0018-9480/85/0800-0693$01.00 ©1985 IEEE

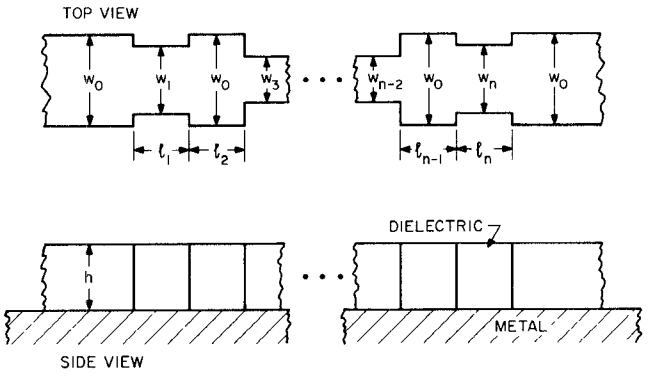

Fig. 1. An "image guide" dielectric waveguide (DW) grating.

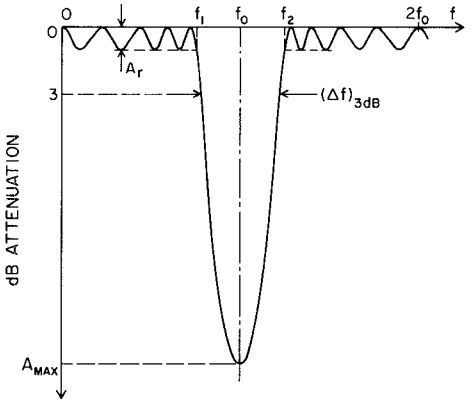

Fig. 2. Definition of a bandstop filter response.

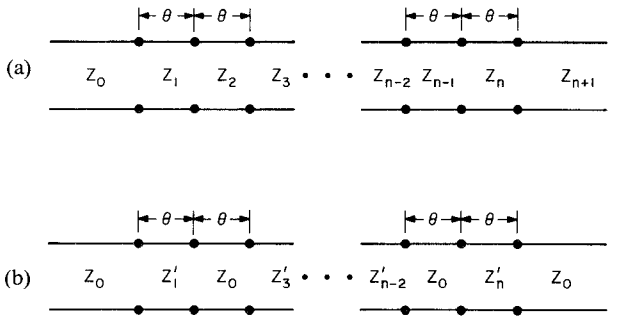

Fig. 3. Transmission-line equivalent circuits for gratings. The circuit at (b) relates to a uniform DW with notches in it.

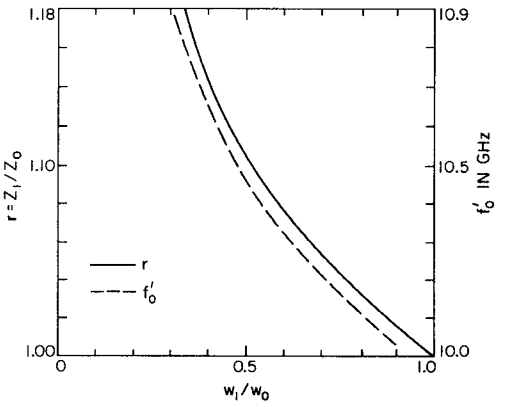

Fig. 4. Measured data for the impedance ratio r and the stopband-center frequency f_0' versus w_1/w_0, which were obtained from tests on uniform gratings.

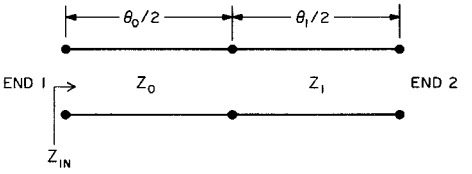

Fig. 5. A fundamental section of an infinitely long uniform grating.

We measured the stopband center frequency f_0' and the mid-stopband attenuation A_{max}. Next, the same measurements were repeated using increased notch depths (reducing w_1/w_0) while keeping l fixed. The impedance ratio r for each w_1/w_0 can be calculated using (1a) and (1b). The data we obtained is shown in Fig. 4, and this data will be used later in realizing a DW bandstop filter. Note that f_0' increases as w_1/w_0 decreases, indicating an increase in average wave velocity as the notches are made deeper. Compensation for this effect is discussed in Section IV.

In order to be able to evaluate the fundamental characteristics of gratings independently from whatever terminations they are going to have, it is desirable to utilize parameters of infinitely long uniform gratings. This can be done in terms of their "image parameters" [5, ch. 3]. Fig. 5 shows the fundamental section of the infinitely long uniform grating to be analyzed. Assuming the network in Fig. 5 is a dissipationless network, we compute the input impedance

$$Z_{in} = \begin{cases} j(X_{oc})_1 \\ j(X_{sc})_1 \end{cases} \qquad (2)$$

where $j(X_{oc})_1$ is the impedance at End 1 of the network with End 2 open-circuited, and $j(X_{sc})_1$ is the impedance at End 1 with End 2 short-circuited. In the stopband, $|(X_{sc})_1| > |(X_{oc})_1|$, and the image attenuation α and the image phase β are given by

$$\alpha = \tanh^{-1}\sqrt{\frac{(X_{oc})_1}{(X_{sc})_1}} \quad \text{nepers/section} \qquad (3)$$

and

$$\beta = (2n-1)\frac{\pi}{2} \quad \text{radians/section} \qquad (4)$$

where

$$T = \text{antilog}_{10}\left(\frac{-A_{max}}{10}\right) \qquad (1b)$$

and n' is the number of Z_1 sections in the equal-line-length equivalent circuit of the uniform grating. A convenient way to obtain design data for gratings with varying notch depths is to make tests on uniform gratings with a range of notch depths. Using this approach, we first made a Rexolite 1422 uniform grating having $\epsilon_r = 2.55$, 40 Z_1 (i.e., notched) sections, $w_0 = 0.5$ in, $l = 0.231$ in, and relatively shallow notches having $w_1/w_0 = 0.875$. The dimensions were so picked that the theoretical stopband center frequency for the grating occurred at 10 GHz as estimated using the effective dielectric constant (EDC) method [4].

where $(2n-1)$ implies an odd multiple. In (2), $(X_{oc})_1$ and $(X_{sc})_1$ are obtained as follows:

$$(X_{oc})_1 = Z_0 \frac{\left(\tan\frac{\theta_0}{2}\right)\tan\frac{\theta_1}{2} - r}{r\tan\frac{\theta_0}{2} + \tan\frac{\theta_1}{2}} \tag{5}$$

and

$$(X_{sc})_1 = Z_0 \frac{\tan\frac{\theta_0}{2} + r\tan\frac{\theta_1}{2}}{1 - r\left(\tan\frac{\theta_0}{2}\right)\tan\frac{\theta_1}{2}} \tag{6}$$

where $r = Z_1/Z_0 > 1$. If $\theta_0 = \theta_1 = \theta = \pi/2$, as for our equal-line-length model at frequency f_0', the above equations reduce to

$$(X_{oc})_1 = Z_0\left(\frac{1-r}{1+r}\right) \tag{7}$$

and

$$(X_{sc})_1 = Z_0\left(\frac{1+r}{1-r}\right). \tag{8}$$

So here (3) becomes

$$\alpha = \tanh^{-1}\left|\frac{1-r}{1+r}\right|_{\theta_0=\theta_1=\theta=\pi/2} \quad \text{nepers/section.} \tag{9}$$

In a previous publication [2], we presented a formula for the fractional bandwidth of the image stopband of a uniform, infinite grating, which is given by

$$\frac{\Delta}{f_0} = \frac{f_b - f_a}{f_0} = \frac{4}{\pi}\sin^{-1}\left(\frac{r-1}{r+1}\right)\Bigg|_{\theta_0=\theta_1=\theta} \tag{10}$$

where Δ is the difference between the upper cutoff frequency f_b and the lower cutoff frequency f_a of the image stopband, and f_0 is the center frequency of the stopband. We can use formulas for α and Δ/f_0 to roughly estimate the number of sections needed and the average value of r that may be needed in the design of practical bandstop filters. Equation (10) does not include the effects of DW dispersion, but at least for the narrow-band case this can be corrected relatively simply by introducing appropriate derivatives of the DW propagation constants. Equation (10) should be divided by

$$D \approx \frac{\left.\dfrac{\dfrac{d\theta_0}{df} + \dfrac{d\theta_1}{df}}{2}\right|_{f=f_0}}{\dfrac{\pi}{2}\dfrac{1}{f_0}} \tag{11a}$$

$$\approx \frac{\left.\dfrac{l_0\dfrac{d\beta_0}{df} + l_1\dfrac{d\beta_1}{df}}{2}\right|_{f=f_0}}{\dfrac{\pi}{2}\dfrac{1}{f_0}} \tag{11b}$$

where θ_0, l_0, and β_0 are for DW of impedance Z_0', and θ_1, l_1, and β_1 are for DW of impedance Z_1.[1] The phase variation of dispersive gratings is more rapid than that of nondispersive gratings so that D is greater than one for dispersive gratings and reduces to one for nondispersive gratings. Thus, the effect of dispersion reduces the stopband width.

It should be noted that Δ in (10) depends only on r and is the stopband width of a uniform, infinite grating. In practical cases of finite, nonuniform gratings with Chebyshev passbands, the stopband width to the equal-ripple points would be somewhat wider than suggested by (10) when (10) is evaluated using a value of r representative of the center part of the grating (where the values of r are largest and nearly uniform). More accurate means for estimating design requirements will be discussed in Sections III and V.

III. Synthesis of Bandstop Filter Prototypes

Our bandstop filter design procedure begins by first obtaining an appropriate transmission-line prototype circuit which uses equal-length line sections as shown in Fig. 3(a). Let us regard Fig. 2 as the attenuation response of the circuit in Fig. 3(a). This idealized attenuation response for structures as in Fig. 3(a) can be defined in terms of Chebyshev polynomials of degree n, the bandwidth, and the maximum stopband VSWR $S_{\max,s}$. An exact general synthesis for half-wave "low-pass" filter prototypes has been presented in [6]. By designing for relatively narrow stopbands, this exact procedure can also be applied to the synthesis of our bandstop filter prototypes. But for cases having a large number of elements, as for narrow-band bandstop filters, the exact method might be too complicated to be practical. Cohn [7] introduced an approximate synthesis procedure for stepped-impedance transformers by considering only first-order reflection effects. This approximate procedure is relatively simple and straightforward so that it can be applied easily to the case of a large number of elements. It works well if the impedance steps are not very large, which is usually the situation for narrow-band bandstop filters of the type under consideration here. We have adapted Cohn's first-order approximations to the bandstop filter problem with some modifications. Our method differs from Cohn's, of course, in that we synthesize bandstop filters rather than bandpass transformers, and that we found it desirable to incorporate the idealized exact expression in (12) for the purpose of helping to fix some of the design parameters. The transducer loss (TL) of the circuit in Fig. 3(a), if exactly designed for a Chebyshev response, is

$$\mathrm{TL} = 10\log_{10}\left[1 + \frac{(S_{\max,s}-1)^2}{4S_{\max,s}}\frac{T_n^2\left(\dfrac{\sin\theta}{\sin\theta_1}\right)}{T_n^2\left(\dfrac{1}{\sin\theta_1}\right)}\right] \quad \text{dB} \tag{12}$$

[1] Note that, as mentioned previously, the actual electrical lengths θ_0 and θ_1 and physical lengths l_0 and l_1 need not be equal, even though we model the grating with equal line lengths.

where $T_n(x)$ is the Chebyshev polynomial of degree n, $S_{\max,s}$ is the maximum stopband VSWR, θ_1 is the electrical length of each section at the lower stopband edge frequency f_1 denoted in Fig. 2, and

$$\theta_1 = \frac{\pi}{2}\frac{f_1}{f_0}. \tag{13}$$

$S_{\max,s}$ can be defined as the product of the junction VSWR's

$$S_{\max,s} = V_1 V_2 \cdots V_{n+1} \tag{14}$$

where V_i is the junction VSWR of the ith junction given by

$$V_i = \left(\frac{Z_i}{Z_{i-1}}\right)^{\pm 1} > 1. \tag{15}$$

In this equation, an appropriate sign has to be chosen in order to have V_i greater than one since the Z_i values alternate up and down. Also, θ_1 is related to the equal-ripple bandwidth $(\Delta f)_{er}$ through the bandwidth ratio p

$$p = \frac{f_2}{f_1} = \frac{2 + \dfrac{(\Delta f)_{er}}{f_0}}{2 - \dfrac{(\Delta f)_{er}}{f_0}} \tag{16}$$

where f_1 and f_2 are the lower and upper stopband edge frequencies, respectively, as shown in Fig. 2, and

$$(\Delta f)_{er} = \frac{f_2 - f_1}{f_0} \tag{17}$$

where f_0 is the center frequency of the stopband. Using (13) and (16), we get

$$\theta_1 = \frac{\pi}{1+p}. \tag{18}$$

The degree n of the Chebyshev polynomial is the same as the number of sections inserted between the terminating impedances Z_0 and Z_{n+1} in Fig. 3(a). We can derive a very useful formula for n using θ_1, $S_{\max,s}$, and the maximum passband VSWR denoted by $S_{\max,p}$. Calculation of the transducer loss at $\theta = \theta_1$, using (12), gives

$$\mathrm{TL}|_{\theta=\theta_1} = 10\log_{10}\left[1 + \frac{(S_{\max,s}-1)^2}{4S_{\max,s}} \frac{1}{T_n^2\left(\dfrac{1}{\sin\theta_1}\right)}\right] \tag{19a}$$

$$= 10\log_{10}\frac{1}{1-|\rho_{\max,p}|^2} \tag{19b}$$

where $|\rho_{\max,p}|$ is the magnitude of the maximum passband reflection coefficient and is given by

$$|\rho_{\max,p}| = \frac{S_{\max,p}-1}{S_{\max,p}+1}. \tag{20}$$

Equation (19b) can also be written in a form similar to (19a), that is,

$$\mathrm{TL}|_{\theta=\theta_1} = 10\log_{10}\left(1 + \frac{|\rho_{\max,p}|^2}{1-|\rho_{\max,p}|^2}\right). \tag{21}$$

After some mathematical manipulation using (19a) and (21), we finally get the following equation:

$$n = \frac{\cosh^{-1} S}{\cosh^{-1}\left(\dfrac{1}{\sin\theta_1}\right)} \tag{22}$$

where

$$S = \frac{S_{\max,s}-1}{2\sqrt{S_{\max,s}}}\sqrt{\left(\frac{S_{\max,p}+1}{S_{\max,p}-1}\right)^2 - 1}. \tag{23}$$

Therefore, if θ_1, $S_{\max,s}$, and $S_{\max,p}$, or equivalently the fractional bandwidth, the maximum stopband attenuation, and the specified passband ripple size, are given, we can calculate the number of sections to be inserted between the two terminating impedances of Z_0 and Z_{n+1} by use of (22) and (23).

It may be well to note at this point that the transmission-line prototype having the response given by (12) does not include the effects of the stopband-width shrinkage that will occur due to dispersion. For this reason, an oversized fractional stopband width should be used in the design of the prototype. These matters will be discussed in Section V.

After we have calculated n for given specifications, we need to calculate the junction VSWR's V_i or the normalized section impedances Z_i. For the approximate synthesis purpose, as done by Cohn for the case of step-transformer, we assume that steps are so small that the reflection interaction between steps can be neglected in the prototype circuit in Fig. 3(a). Then, the total reflection coefficient of the bandstop filter prototype referred to at the center of the filter structure is expressed as follows:

$$\rho = A_1 e^{j n\theta} - A_2 e^{j(n-2)\theta} + \cdots + (-1)^n A_{n+1} e^{-jn\theta} \tag{24}$$

where the A_i's are the junction reflection coefficient *magnitudes*, which are given by

$$A_i = \pm\frac{Z_i - Z_{i-1}}{Z_i + Z_{i-1}} > 0, \qquad \text{for } i = 1,2,\cdots,n+1. \tag{25}$$

The magnitude of the step reflections are assumed to be symmetrical, i.e., $A_1 = A_{n+1}$, $A_2 = A_n$, etc. Therefore, for n odd

$$\rho = j\sum_{k=0}^{(n-1)/2}\left[(-1)^k 2A_{k+1}\sin(n-2k)\theta\right] \tag{26}$$

and for n even

$$\rho = \begin{cases} A_1, & \text{when } n = 0 \\ \displaystyle\sum_{k=0}^{(n-2)/2}(-1)^k 2A_{k+1}\cos(n-2k)\theta + (-1)^{(n/2)}A_{\frac{n+2}{2}}, & \text{when } n \geq 2 \end{cases} \tag{27}$$

In order to obtain Chebyshev passbands, ρ in (26) and (27) is forced to be equal to a Chebyshev polynomial $\alpha T_n(x)$, where α is a constant which need not be explicitly evaluated

and

$$x = \frac{\sin\theta}{\sin\theta_1}. \tag{28}$$

For $n = 0$, 1, and 2

$n = 0$:

$$\rho = \alpha T_0(x) = \alpha = A_1$$
$$\therefore A_1 = \alpha$$

$n = 1$:

$$\rho = \alpha T_1(x) = \alpha x = j2A_1 \sin\theta = j2A_1 x \sin\theta_1$$
$$\therefore A_1 = \frac{\alpha}{j2\sin\theta_1}$$

$n = 2$:

$$\rho = \alpha T_2(x) = \alpha(2x^2 - 1) = 2\alpha x^2 - \alpha = 2A_1\cos 2\theta - A_2 = 2A_1(1 - 2x^2\sin^2\theta_1) - A_2 = -4A_1 x^2 \sin^2\theta_1 + 2A_1 - A_2$$
$$\therefore A_1 = -\frac{\alpha}{2\sin^2\theta_1} \quad A_2 = -\frac{\alpha}{\sin^2\theta_1} + \alpha.$$

We keep going until the desired value of n is reached. Similarly to Cohn [7], this procedure can be tabulated and generalized as shown in Table I.

The following points should be noted.

1) In the upper left-hand corner of the table, always insert a number for α. Pick $\alpha = 2$ for simplicity.

2) With $\alpha = 2$, in the second column, second row, always insert

$$x_0 = \frac{1}{\sin\theta_1}. \tag{29}$$

3) To find an additional entry in the first column, multiply the element on the right just above by $2x_0$ and then subtract the element in the second row directly above the entry to be found.

4) To find an additional entry in any other column, add the elements on the left and right just above and multiply by x_0, and then subtract the element in the second row directly above the entry to be found.

5) Where an element is absent, assume it to be zero.

6) The A_i values will appear in every other space in each row, and the elements on the principal diagonal of the array constructed in this manner are values for A_1 for different values of n.

7) The values of A_i obtained using the method of Table I may differ from those obtained directly from Chebyshev polynomials by a common factor. However, since we need only the ratios of the A_i, it does not matter.

Following the above procedure, we are able to determine the following junction reflection-coefficient magnitude ratios:

$$A_1 : A_2 : \cdots : A_{n+1} = a_1 : a_2 : \cdots : a_{n+1} \tag{30}$$

where $a_i = A_i/A_1$. Assuming the impedance steps are small,

TABLE I
COMPUTATION OF A_i RATIOS

n=0	α			
n=1		$\frac{\alpha}{2\sin\theta_1}$		
n=2	$\frac{\alpha}{\sin^2\theta_1} - \alpha$		$\frac{\alpha}{2\sin^2\theta_1}$	
etc.				

(25) can be written approximately as

$$A_i \approx \pm\frac{1}{2}\ln\frac{Z_i}{Z_{i-1}} > 0. \tag{31}$$

Plugging (31) into (30) and performing some manipulation gives

$$\left|\ln\frac{Z_i}{Z_{i-1}}\right| = \begin{cases} \dfrac{a_i\left(\ln\dfrac{Z_1}{Z_0} + \ln\dfrac{Z_1}{Z_2} + \cdots + \ln\dfrac{Z_n}{Z_{n+1}}\right)}{a_1 + a_2 + \cdots + a_{n+1}}, & \text{for } n \text{ odd} \\ \dfrac{a_i\left(\ln\dfrac{Z_1}{Z_0} + \ln\dfrac{Z_1}{Z_2} + \cdots + \ln\dfrac{Z_{n+1}}{Z_n}\right)}{a_1 + a_2 + \cdots + a_{n+1}}, & \text{for } n \text{ even} \end{cases}$$
$$= \frac{a_i(\ln V_1 + \ln V_2 + \cdots + \ln V_{n+1})}{a_1 + a_2 + \cdots + a_{n+1}} = \frac{a_i \ln(V_1 V_2 \cdots V_{n+1})}{a_1 + a_2 + \cdots + a_{n+1}} = \frac{a_i \ln(S_{\max,s})}{a_1 + a_2 + \cdots + a_{n+1}}. \tag{32}$$

Knowing the a_i by use of Table I and (30), and knowing $S_{\max,s}$, we can then compute all the ratios Z_i/Z_{i-1} by use of (32).

As shown above, the normalized impedance of each section is obtained using the first-order approximation, while the number of sections needed is calculated using the exact formula of (22). We computed the attenuation responses of some idealized designs using (12) and compared them with responses of approximate designs obtained using the first-order theory. They agreed very well in the maximum attenuation $A_{\max}$, but showed big differences both in the equal-ripple bandwidth and in the ripple size. An approximate design showed 20-dB maximum attenuation, 18-percent equal-ripple bandwidth, and 0.000065-dB ripple as compared to a 20-dB maximum attenuation, 10-percent bandwidth, and 0.00087-dB ripple design objective. These discrepancies in the equal-ripple bandwidth and the ripple

size are believed to have come from neglecting the higher order reflections and from the approximation used in (31).

In order to reduce such errors, some modifications were made in the design procedure. From (12), it can be shown that the input reflection coefficient for an exact Chebyshev bandstop design is

$$\rho_e = \frac{\dfrac{S_{\max,s}-1}{2\sqrt{S_{\max,s}}}\dfrac{T_n\left(\dfrac{\sin\theta}{\sin\theta_1}\right)}{T_n\left(\dfrac{1}{\sin\theta_1}\right)}}{\sqrt{1+\dfrac{(S_{\max,s}-1)^2}{4S_{\max,s}}\dfrac{T_n^2\left(\dfrac{\sin\theta}{\sin\theta_1}\right)}{T_n^2\left(\dfrac{1}{\sin\theta_1}\right)}}}. \tag{33}$$

The corresponding approximate equation which is consistent with ignoring higher order reflections is

$$\rho_a = \frac{1}{2}\ln(S_{\max,s})\frac{T_n\left(\dfrac{\sin\theta}{\sin\theta_1}\right)}{T_n\left(\dfrac{1}{\sin\theta_1}\right)}. \tag{34}$$

(Equation (34) is analogous to [7, eq. (36)] for the step-transformer case.) A correction was introduced by making the ripple sizes of (33) and (34) the same at the band edge. By replacing θ_1 with θ_1' in (34) and setting $\rho_a|_{\theta=\theta_1'} = \rho_e|_{\theta=\theta_1}$, we get

$$\theta_1' = \sin^{-1}\left[\frac{1}{\cosh\left(\dfrac{\cosh^{-1}S'}{\cosh^{-1}S}\cosh^{-1}\left(\dfrac{1}{\sin\theta_1}\right)\right)}\right] \tag{35}$$

where S is given in (23), θ_1 is given in (18), and

$$S' = \frac{\ln(S_{\max,s})}{S_{\max,p}-1}. \tag{36}$$

Parameter θ_1' calculated using (35) is then used in place of θ_1 to generate Table I, that is, in (29), θ_1' replaces θ_1.

Application of this approach to examples showed that use of (35) in (29) resulted in a greatly improved accuracy in the passband ripple (the decibel passband ripple was typically within a factor of 1.1 or better of the specified decibel value instead of being off by more than a factor of ten in some cases). However, the fractional bandwidth at the equal-ripple level was only moderately improved. In the previously cited example having a 10-percent equal-ripple bandwidth objective, the use of (35) resulted in a 15-percent equal-ripple bandwidth as compared with 18-percent when (35) was not used. Importantly, the agreement at the 3-dB bandwidth level was much better. For the same example, the stopband width at the 3-dB level for an exact design was 7.2 percent, for an approximate design obtained utilizing (35), the 3-dB stopband width was 7.8 percent, while, without the correction in (35), the width was 8.7 percent. In all cases, the desired peak attenuation was obtained with high accuracy.

The 3-dB bandwidth $(\Delta f)_{3\text{ dB}}$ can be well estimated using (12). Let $\theta_{3\text{ dB}}$ be the electrical length of each section at the lower 3-dB frequency of the stopband; then from (12)

$$\theta_{3\text{ dB}} = \sin^{-1}\left[(\sin\theta_1)\cosh\left[\frac{1}{n}\cosh^{-1}\left\{\frac{2\sqrt{S_{\max,s}}}{S_{\max,s}-1}\cosh\left(n\cosh^{-1}\frac{1}{\sin\theta_1}\right)\right\}\right]\right] \tag{37}$$

where θ_1 is given in (18), and

$$\frac{(\Delta f)_{3\text{ dB}}}{f_0} = 2 - \frac{4\theta_{3\text{ dB}}}{\pi}. \tag{38}$$

The prototype circuits for bandstop filters of the form in Fig. 3(a) typically have increasing values of $Z_k|_{k=\text{odd}}$ as one moves towards the center of the filter and decreasing values of $Z_k|_{k=\text{even}}$ as one moves towards the center of the filter. This is not very practical for DW gratings. A more practical form is shown in Fig. 3(b), where all of the even-numbered sections have been replaced by line sections of impedance Z_0, while the odd-numbered sections are all of an impedance higher than Z_0. This configuration is then amenable to being realized as a uniform DW with notches cut into it to create the higher impedance line sections. An approximate procedure for converting designs as in Fig. 3(a) to the form in Fig. 3(b) is to make

$$Z_l'|_{l=\text{odd}} = Z_0\left(\frac{\dfrac{Z_l}{Z_{l-1}}+\dfrac{Z_l}{Z_{l+1}}}{2}\right) \tag{39a}$$

$$Z_l'|_{l=\text{even}} = Z_0. \tag{39b}$$

This procedure was found to affect the responses of trial designs very little. For example, a design having a 0.00087-dB ripple objective, the ripples near cutoff are a little large but taper down to be less than the design objective at low frequencies, as are shown in Fig. 8(b). The approximation has virtually no effect on the stopband.

It is helpful as a design guide if we have theoretical plots showing the relations between the number of grating notches and the equal-ripple bandwidth, and also between the maximum impedance ratio $r_{\max}$ (which is the normalized impedance at the center of the grating) and the bandwidth, for given maximum stopband decibel attenuation $A_{\max}$ and passband decibel ripple size A_r. Using (22) and the generalized synthesis procedure in Table I, we made theoretical plots in Fig. 6. Fig. 6(a) is the plot for a bandstop filter prototype with $A_{\max} = 20$ dB and $A_r = 0.00087$ dB, which gives a minimum of 37-dB return loss in the passbands, such as might be a desirable goal if filters

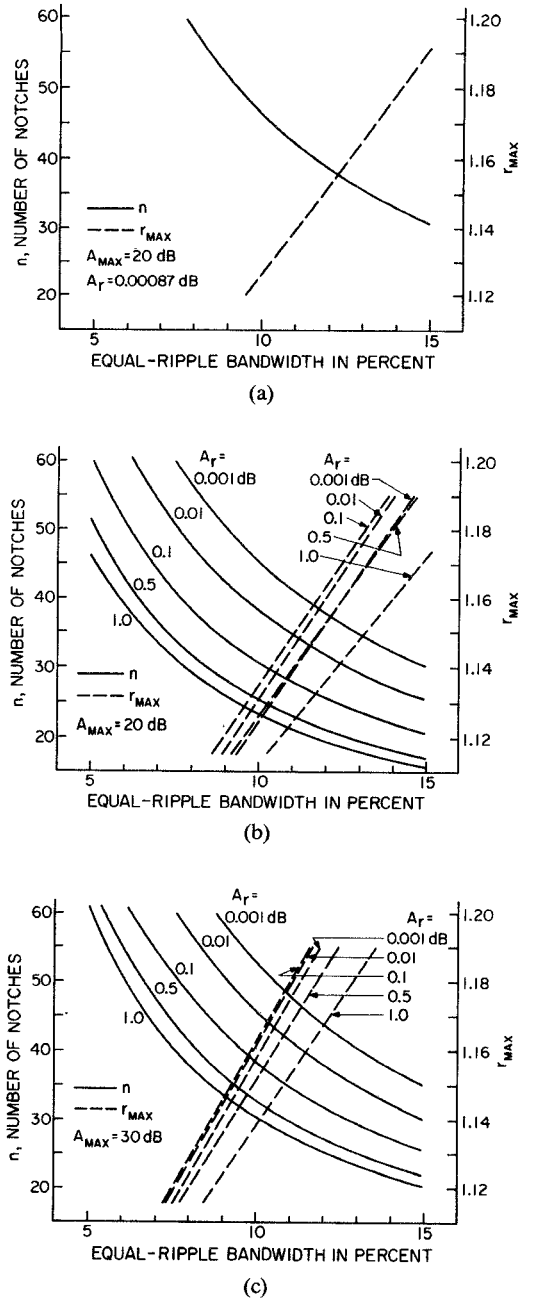

Fig. 6. Theoretical plots to be used in estimating the number of notches n and the maximum impedance ratio r_{max} required in a bandstop filter prototype having a given equal-ripple bandwidth, passband ripple A_r, and maximum attenuation A_{max}.

like this are used as gratings in a bandpass filter like that in Fig. 11. Fig. 6(b) and (c) are generalized plots for $A_{max} = 20$ dB and $A_{max} = 30$ dB, respectively, with A_r as a parameter.

IV. Realization of a Bandstop Filter from a Transmission-Line Prototype

In order to realize the prototype circuit in Fig. 3(b) with a uniform DW having notches cut in it, the length, width, and location of each notch must be determined. Using the measured design data such as that shown in Fig. 4, we can determine the value of w_i/w_0 (hence, the required notch

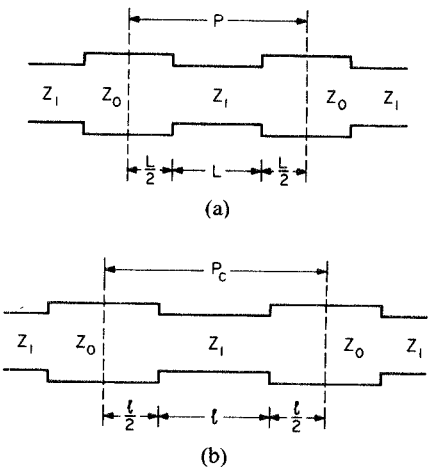

Fig. 7. At (a) is shown a period of a uniform grating whose stopband-center frequency is f_0'. At (b) is shown a period whose dimensions are altered to give a stopband-center frequency f_0.

depth) for a given impedance ratio $r_i = Z_i'/Z_0$ (see Fig. 3(b)). Therefore, if we fix w_0, the w_i required for notch section i can be determined knowing r_i of the corresponding prototype section. Next, we have to determine the exact length of each line section in order for every period of the grating to be resonant at the same frequency f_0 (which is the center frequency of a bandstop filter) regardless of the notch depth. By a period of the circuit in Fig. 3(b) we mean a section composed of a given notch plus half of the Z_0 section on each side as in Fig. 7. Using the design data in Fig. 4 once again, we can read the value of the stopband center frequency f_0' for a given notch depth (i.e., w_1/w_0 value). We need to adjust every period of the circuit in Fig. 3(b) so as to have the same resonant frequency $f_0' = f_0$ (the desired stopband center frequency of the filter). This length correction scheme is shown in Fig. 7, where P is the period of the test grating and P_c is the period of the length-corrected grating section. Now, let β_{ave} be the average propagation constant at the resonant frequency f_0' of the test grating with the desired w_1/w_0 value. Then

$$\beta_{ave} P|_{f=f_0'} = \pi \quad \text{radians} \tag{40}$$

where β_{ave} is defined as

$$\beta_{ave} = \frac{\beta_0 + \beta_1}{2} \tag{41}$$

and β_0 and β_1 are the propagation constants of Z_0 and Z_1 sections, respectively. The parameter β_{ave} varies from one section of a filter structure to another because of the varying notch depths. For a given section of the structure with average phase constant β_{ave}, and by using a Taylor series expansion, we obtain

$$\beta_{ave} P|_{f=f_0} \approx \beta_{ave} P|_{f=f_0'} + \left.\frac{d(\beta_{ave} P)}{df}\right|_{f=f_0'} (f_0 - f_0')$$

$$\approx \pi + \left.\frac{d(\beta_{ave} P)}{df}\right|_{f=f_0'} (f_0 - f_0'). \tag{42}$$

Now let P_c be the corrected length such that at the desired

center frequency f_0

$$\beta_{ave}P_c|_{f=f_0} = \pi \quad \text{radians.} \tag{43}$$

Then, from (42) and (43)

$$\frac{P_c}{P} = \frac{\beta_{ave}P_c|_{f=f_0}}{\beta_{ave}P|_{f=f_0}} = \frac{\pi}{\beta_{ave}P|_{f=f_0}}$$

$$= \frac{\pi}{\pi + \left.\dfrac{d(\beta_{ave}P)}{df}\right|_{f=f_0'}(f_0 - f_0')}. \tag{44}$$

In our trial design, the quantities $d(\beta_{ave}P)/df|_{f=f_0'}$ in (44) were evaluated using the effective dielectric constant (EDC) method, and corrected periods P_c were computed for the entire structure. The corrected length l for each period (see Fig. 7(b)) was then scaled to bring the entire structure into synchronism at the same frequency f_0.

V. Concerning the Correction of Design Bandwidth to Allow for Dispersion

In the synthesis of a prototype as in Section III, it is necessary to use an oversized stopband width because this width will shrink due to dispersion in the DW filter. A simple way to estimate dispersion in the DW filter is to estimate the nominal impedance ratio r in the center part of the filter where the values of r are largest and nearly uniform. By regarding the maximum impedance ratio r_{max} (which is the impedance ratio at the center of the filter) as the nominal ratio in the center part of the filter, we developed a procedure to estimate r_{max} from the design specifications. This procedure used some of the concepts in [9] where sections of a lumped-element, low-pass filter prototype designed on the insertion-loss basis were related to corresponding transmission-line filter sections with the aid of image analysis. Following the idea in [9], we can derive an expression for r_{max} given by

$$r_{max} = \frac{(2-M)+2\sqrt{1-M}}{M} \tag{45}$$

where

$$M = \frac{4}{g_k g_{k+1}(\omega_1')^2}\sin^2\left[\frac{\pi}{2}\left(1 - \frac{(\Delta f)_{er}}{2f_0}\right)\right] \tag{46}$$

where g_k and g_{k+1} are the two center elements of a low-pass prototype [5, ch. 4] having the desired passband ripple and a number of elements n obtained using an estimated θ_1 value in (22). The parameter ω_1' is the cutoff frequency of the low-pass prototype. After estimating r_{max} by use of (45) and (46), the notch and spacing dimensions in the center of the filter can be estimated with the aid of Fig. 4 and (44). Having estimated dimensions for the dominant part of the grating, an estimated value of the parameter D can be obtained using (11b) and the EDC method [4]. For purposes of designing the transmission-line prototype as discussed in Section III, the desired fractional bandwidth should be multiplied by D to compensate for the stopband-width shrinkage that will result from dispersion.

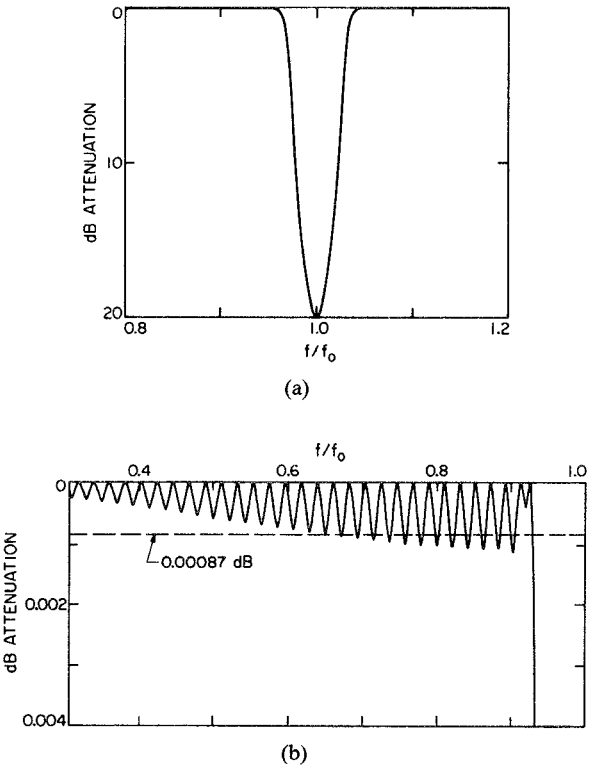

Fig. 8. (a) The computed attenuation characteristics of a trial grating design including correction for dispersion. (b) The solid line shows the computed passband ripple characteristic for a design of the form in Fig. 3(b).

As an example, for the previously discussed trial design with 0.00087-dB passband ripple, by (45) and (46) we estimated $r_{max} = 1.117$, while r_{max} obtained from the whole synthesis was 1.125. From this estimated r_{max} of 1.117 and the design data in Fig. 4, $w_1/w_0 = 0.46$ and $f_0' = 10.53$ GHz were obtained. Then using the length correction equation of (44) for $P = 2L = 0.462$ in and $f_0 = 10$ GHz, we got $P_c/P = 1.071$. At this point, the lengths and the widths of the center fundamental section were estimated. Finally, D in (11b) was calculated. The derivatives in (11b) were calculated using the EDC method [4] and we obtained $D = 1.321$. The prototype had a 3-dB stopband width of 7.82 percent. Therefore, the dispersion-corrected 3-dB stopband width for the DW bandstop filter can be estimated as 7.82 (percent)/1.321 = 5.92 percent. A more complete calculation using a linear correction for dispersion computed for each individual section gave 5.93 percent, while the measured stopband width at the 3-dB level was 6.05 percent. The approximate procedure for estimating the dispersion-corrected bandwidth seems to work very accurately.

VI. Experimental Results

Using the realization procedure mentioned in Section IV, a DW bandstop filter was fabricated whose theoretical responses were computed to be as shown in Fig. 8(a) and (b). The DW utilized Rexolite 1422, which has $\epsilon_r = 2.55$, and the guide was 0.4-in high by 0.5-in wide with notches as in Fig. 1 ranging from 0.021-in deep at the ends to

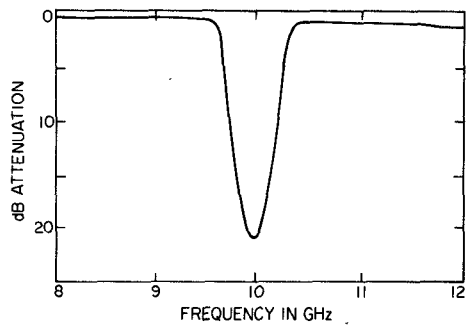

Fig. 9. The measured attenuation characteristic for the same design as in Fig. 8(a) and (b).

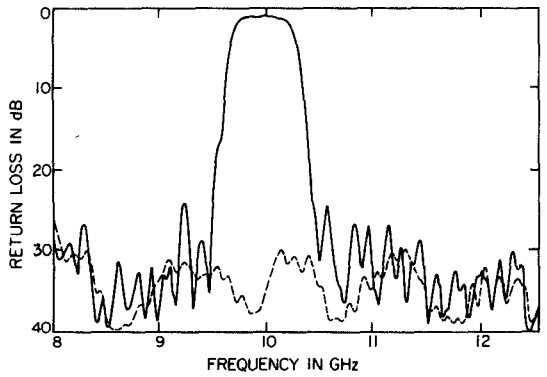

Fig. 10. The solid line shows the measured return-loss characteristic for the same bandstop grating as in Fig. 9. The dashed line suggests the limit of sensitivity of the measurement system.

0.141-in deep at the center of the grating. Fig. 9 shows the measured attenuation, which is in excellent agreement with the theoretical response. The floor attenuation in Fig. 9 is due to the loss of the mode launchers at the ends and the dissipative loss of the guide itself. The measured peak attenuation is almost exactly 20 dB above the attenuation floor, while the 3-dB stopband bandwidth is about 6.05 percent as compared to a theoretically estimated 5.92 percent, as mentioned in Section V. Fig. 10 shows the measured return loss. The dashed line shows the return loss of a load on the dielectric waveguide without a grating and suggests the measurement limits of the test setup, which included a mode transducer from metal guide to DW. The solid line shows the measured return loss of the filter, and it is seen to have stronger sidelobes than the desired -37-dB maximum. Computer studies suggest that errors in the desired very low sidelobes could easily be due to some lack of synchronism between the various parts of the grating having different notch depths.

VII. Application to Bandpass Filters

Precision bandstop grating designs of this sort also have potential application for use in bandpass filters. Fig. 11 shows a bandpass filter made with a 3-dB coupler and two gratings with loads at their right ends. It can be shown that when the gratings are reflecting, power entering the coupler at port 1 will emerge at port 2 yielding a passband. However, when the gratings are not reflecting, power entering at port 1 will pass through the gratings and be absorbed by the loads at the right, thus creating a stopband with respect to transmission from port 1 to port 2. Matthaei *et al.* [2] have discussed the fundamentals of a bandpass filter technique which uses parallel gratings with coupling between them. However, that technique appears to be most practical for filters having bandwidths of the order of one percent since, when using that technique, the passband width of the filter must be considerably less than the image stopband width of the gratings. It can be shown that the structure in Fig. 11 has potential application for passband widths up into the 5–10-percent range. This is because, for the structure in Fig. 11, the passband for transmission from port 1 to port 2 corresponds to the full width of the grating stopband.

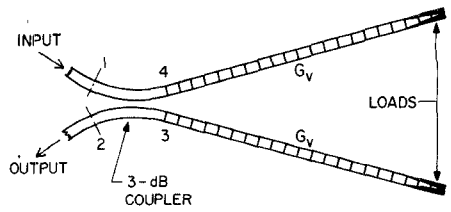

Fig. 11. A bandpass filter formed from two DW bandstop gratings plus a DW 3-dB coupler.

VIII. Conclusions

Precision design and realization procedures have been obtained for DW bandstop filters. The design process utilized a transmission-line prototype filter which was designed using various simplifying approximations. The resulting prototypes gave the desired passband ripple and the desired attenuation characteristic at the 3-dB level or above with good accuracy, but tended to give an oversized stopband width at the equal-ripple level. The results of a trial design with extremely demanding design objectives yielded an attenuation characteristic which was in most respects in excellent agreement with the objective. A simple dispersion correction method which uses the combination of the image and insertion-loss points of view has been presented and it worked very well. The much more sensitive return-loss characteristic did not meet the very difficult -37-dB sidelobe objective as well, but it is believed that by use of more precise design data appreciably more precise return loss should be possible.

References

[1] T. Itoh, "Applications of gratings in a dielectric waveguide for leaky-wave antennas and band-reject filters," *IEEE Trans. Microwave Theory Tech.*, vol. MTT-25, pp. 1134–1138, Dec. 1977.

[2] G. L. Matthaei, D. C. Park, Y. M. Kim, and D. L. Johnson, "A study of the filter properties of single and parallel-coupled dielectric-waveguide gratings," *IEEE Trans. Microwave Theory Tech.*, vol. MTT-31, pp. 825–835, Oct. 1983.

[3] D. C. Park, G. L. Matthaei, and M. S. Wei, "Dielectric waveguide grating design for bandstop and bandpass filter applications," in *1984 IEEE MTT-S Int. Microwave Symp. Dig.*, pp. 202–204.

[4] W. V. McLevige, T. Itoh, and R. Mittra, "New waveguide structures for millimeter-wave and optical integrated circuits," *IEEE Trans. Microwave Theory Tech.*, vol. MTT-23, pp. 788–794, Oct. 1975.

[5] G. L. Matthaei, L. Young, and E. M. T. Jones, *Microwave Filters Impedance-Matching Networks, and Coupling Structures*. New York: McGraw-Hill, 1964; Dedham, MA: Artech House, 1980.
[6] R. Levy, "Tables of element values for the distributed low-pass prototype filters," *IEEE Trans. Microwave Theory Tech.*, vol. MTT-13, pp. 514–536, Sept. 1965.
[7] S. B. Cohn, "Optimum design of stepped transmission-line transformers," *IRE Trans. Microwave Theory Tech.*, vol. MTT-3, pp. 16–21, Apr. 1955.
[8] R. E. Collin, "Theory and design of wide-band multisection quarter-wave transformers," *Proc. IRE*, vol. 43, pp. 179–185, Feb. 1955.
[9] G. L. Matthaei, "Design of wide-band (and narrow-band) band-pass microwave filters on the insertion loss basis," *IRE Trans. Microwave Theory Tech.*, vol. MTT-8, pp. 580–593, Nov. 1960.

✠

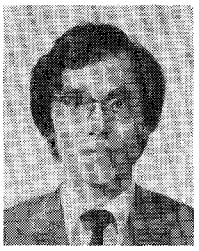

Dong Chul Park (S'81–M'85) was born in Pusan, Korea, in 1952. He received the B.S. degree in electronics from Seoul National University in 1974, the M.S. degree from Korea Advanced Institute of Science and Technology in 1976, and the Ph.D. degree from the University of California, Santa Barbara, in 1984.

Since 1976, he has been working at Chungnam National University, where he is an Assistant Professor, in Daejon, Korea. From 1977 to 1978, he was a Visiting Scholar at Ruhr University, Bochum, West Germany, where he worked on integrated optics. From 1981 to 1984, he was in the Ph.D. program at the University of California, Santa Barbara, on a Fulbright Grant. His research interests are in microwave and millimeter-wave devices, electromagnetic-field theory, and integrated optics.

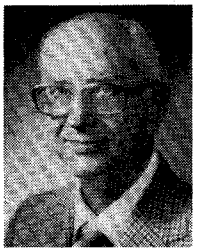

George L. Matthaei (S'49–A'52–M'57–F'65) was born August 28, 1923, in Tacoma, WA. He received the B.S. degree from the University of Washington in 1948, and the Ph.D. degree from Stanford University in 1952.

From 1951 to 1955, he was on the faculty of the University of California, Berkeley, where he was an Assistant Professor, and his specialty was network synthesis. From 1955 to 1958, he was engaged in system analysis and microwave component research at the Ramo-Wooldridge Corporation. From 1958 to 1964, he was at the Stanford Research Institute, where he was engaged in microwave device research and became Manager of the Electromagnetic Techniques Laboratory in 1962. In July 1964, he joined the Department of Electrical Engineering at the University of California, Santa Barbara, where he is a Professor. He is the author of numerous papers, coauthor of the book *Microwave Filters, Impedance-Matching Networks and Coupling Structures*, and a contributer to several other books. His current interests are in the areas of microwave and millimeter-wave passive and active circuits.

Dr. Matthaei is a member of Tau Beta Pi, Sigma Xi, and Eta Kappa Nu. He was the winner of the 1961 Microwave Prize of the IEEE MTT Group. In 1984, he received an IEEE Centennial Medal.

✠

Mu Sheng Wei was born in Jiangsu, China, in October 1942. He graduated from Harbin Engineering Institute, Heilongjiang, China, in 1965.

After graduation, he was with Zhongyuan Research Institute of Electronics Technology, Zhumadian, Henan, China, where he was engaged in research on solid-state microwave sources, frequency multipliers, and atomic frequency standards. Since May 1983, he has been a Visiting Scholar in the Department of Electrical and Computer Engineering, University of California at Santa Barbara. His current research interest is mainly in the applications of dielectric waveguide circuits for millimeter-wave frequencies.